Probing the Topology of the Glycine Receptor by Chemical Modification Coupled to Mass Spectrometry†

John F. Leite‡ and Michael Cascio*

Department of Molecular Genetics and Biochemistry, School of Medicine, University of Pittsburgh, Pittsburgh, Pennsylvania 15261

Received October 26, 2001; Revised Manuscript Received February 17, 2002

ABSTRACT: Tetranitromethane (TNM), a small aqueous reagent that specifically modifies solvent-accessible tyrosine residues to *o*-nitrotyrosine, was used to probe the topology of the GlyR. Homomers of human α1 GlyR were recombinantly expressed via a baculovirus system, affinity-purified, and reconstituted in lipid vesicles of defined composition. The native-like reconstituted receptors were then reacted with TNM, and GlyR reaction products were isolated by SDS−PAGE. After proteolytic digestion, TNM-labeled residues were identified using mass spectrometry by observing the mass shift corresponding to the nitrate moiety. In this manner, we have identified TNM modifications of tyrosine residues at positions 24, 75, 78, 161, 223, and 228 in the receptor. Of significance, nitrations at Tyr 223 and Tyr 228 occur within the first putative transmembrane helix (M1) of the receptor, and their labeling suggests a nonhelical secondary structure for M1 for the glycine receptor. In a previously published report [Leite et al. (2000) *J. Biol. Chem. 275*, 13683], we also identified proteolytic cleavage sites within M1. Taken together, these studies support a topological model where the "historical" M1 segment cannot be entirely α-helical and may contain an extramembranous surface loop. Furthermore, we have also identified a tyrosine modification (Tyr 161) within a region of the N-terminal domain critical in agonist and antagonist binding.

The glycine receptor (GlyR)[1] is a major inhibitory neurotransmitter receptor in the mammalian spinal cord and lower brain. Upon binding glycine, the channel opens and transiently fluxes chloride ions, thus increasing the electrochemical membrane potential. This function is crucial in coordinating proper regulation of synaptic signaling. *In vivo*, GlyR is a heteropentameric assembly of α and *β* subunits. However, functionally native-like homopentamers can be obtained by expressing α1 subunits (*1*, *2*). Our laboratory has exploited the baculovirus system as a means of expressing recombinant GlyR (*3*). Affinity-purified GlyR (by 2-aminostrychnine−agarose), reconstituted in lipid vesicles, has been shown to retain pharmacologically native-like activity by mass flux assays as well as single-channel electrophysiology (*4*). The GlyR is a member of the nicotinicoid superfamily of ligand-gated ion channels. This family also includes receptors for acetylcholine, *γ*-aminobutyric acid (GABA), and serotonin. Given the high degree of sequence homology between subunits of various nicotinicoid receptors, we consider the reconstituted homomeric GlyR α1 to be a paradigmatic structural model for the superfamily in general.

Historically, the accepted topology of the GlyR, as well as the remainder of the nicotinicoid ion channels, is described as having a large amino-terminal domain tethered to four transmembrane (TM) α-helices (M1−M4), with a large intracellular loop between M3 and M4 and an extracellular C-terminus. The large intracellular loop between M3 and M4 is of variable length among members of the superfamily and is the least conserved (see ref *5* for review). This loop contains putative phosphorylation sites and contains target sites for cytoplasmic proteins such as rapsyn for AchR (*6*) and gephyrin for GlyR (*7*), which are believed to act in targeting and clustering of the channels. Site-directed mutagenesis studies have identified M2 as the pore-forming domain (for review, see ref *8*). Several studies utilizing chemical modification and/or systematic cysteine mutagenesis have identified periodicities in the labeling of M2 and M4 which suggest that they do indeed adopt an α-helical fold; similar studies have suggested that M1 adopts a nonhelical fold (*9*−*13*). Several spectroscopic studies have reported results that are inconsistent with the four TM α-helix model. Specifically, circular dichroism (CD) studies from our laboratory have demonstrated that the α-helical content of α1 GlyR homopentamers cannot accommodate four TM α-helices (*4*). Spectroscopic studies of the nicotinic acetylcholine receptor (nAchR), using FTIR (*14*, *15*) and IR (*16*), suggest that this receptor's TM domains are also composed

† This work was supported by NIH Grant GM51911.

* Corresponding author. Telephone: (412) 648-9488. Fax: (412) 624-1401. E-mail: Cascio@pitt.edu.

‡ Current address: Division of Biology, M/C 156-29, California Institute of Technology, Pasadena, CA 91125.

[1] Abbreviations: GlyR, glycine receptor; AchR, nicotinic acetylcholine receptor; GABAR, *γ*-aminobutyric acid receptor; C-terminus, carboxy terminus; N-terminus, amino terminus; TM, transmembrane; FTIR, Fourier transform infrared; IR, infrared; MS, mass spectrometry; MALDI-TOF, matrix-assisted laser desorption time of flight; ESI, electrospray ionization; HPLC, high-performance liquid chromatography; TNM, tetranitromethane; UV, ultraviolet; KP_i, potassium phosphate; KCl, potassium chloride; EDTA, ethylenediaminetetraacetic acid; EGTA, ethylene glycol bis(2-aminoethyl)-*N*,*N*,*N*′,*N*′-tetraacetic acid; DTT, dithiothreitol; SDS−PAGE, sodium dodecyl sulfate−polyacrylamide gel electrophoresis.

10.1021/bi015895m CCC: $22.00 © 2002 American Chemical Society
Published on Web 04/20/2002

of a mixture of α-helices as well as β-strands, though the exact composition remains controversial. Cryoelectron microscopy imaging studies of tubular arrays of nAchR have been only able to identify the single M2 TM α-helix per subunit (*17*, *18*). In other studies from our laboratory, mass spectrometry analysis of soluble and membrane-associated GlyR peptides generated by limited proteolysis of reconstituted receptors provided experimental evidence which was inconsistent with the "historical" four TM topological model (*5*). Specifically, proteolytic cleavages were detected within TM1 and TM3 that should have been inaccessible to proteolytic enzymes if these segments were transmembrane helices. In addition, the length of some membrane-associated fragments (224−234 of M1 and 285−300 of M3) was insufficient to accommodate membrane-spanning α-helices which must be at least 20 residues in length to span the ∼30 Å of the hydrocarbon interior of the bilayer.

In our previous probing of GlyR structure, the topology of the receptor was assessed by determining the accessibility of the peptide backbone to cleavage by proteolytic enzymes. These aqueous proteolytic enzymes are large, bulky molecules, and steric effects might have played a role in restricting the frequency of cleavages at specific sites. Small, aqueous agents which target specific side-chain moieties of the protein may provide additional data to more finely map topology. Tetranitromethane (TNM), a small, water-soluble tyrosine modification reagent, was used in this study to probe the accessibility of Tyr in reconstituted human α1 GlyR. The reaction of TNM with tyrosine under alkaline conditions results in *o*-nitrotyrosine, which shifts Abs_{max} to 428 nm (*19*) and also mass shifts the Tyr residue, adding an additional nitrate group (+45 Da). Tyrosine side chains may be expected to reside in many different microenvironments. These side chains are preferentially enriched in the interfacial region of the bilayer (i.e., with the lipid headgroups). They might also be on the surface of the protein. In both of these cases, the Tyr may be accessible for TNM modification. However, if the Tyr resides in the interior of the bilayer (i.e., at the depth of the acyl chains of the lipids) or in the hydrophobic core of a globular domain, they would be inaccessible to TNM. Thus TNM accessibility provides information that may be used to map the topology of the receptor.

In analogous studies of bacteriorhodopsin, a seven TM helix membrane protein, TNM has been utilized as a topological probe to identify solvent-accessible tyrosine residues (*20*, *21*). Utilizing subsequent high-resolution data from crystallographic studies (*22*), we can retrospectively evaluate the efficacy of TNM as a tool in the topological analysis of BR. TNM was able to specifically modify solvent-accessible tyrosine residues, including tyrosines in the interfacial region of the membrane, aligned with phospholipid headgroups. All tyrosines embedded at the level of the acyl chains remained unmodified. Probing solvent-accessible tyrosines may be particularly useful in examining the topology of membrane proteins in general since aromatic residues, including tyrosine, play an important role in the partitioning properties of TM domains due to their hydrophobicity and propensity to define the ends of TM regions due to their favorable free energies at the membrane−solvent interface (*23*).

While many chemical techniques for labeling specific moieties of proteins are known and widely available, mapping the site(s) of modification had been problematic in studies of proteins of limited abundance. However, recent advances in mass spectrometric technologies have afforded investigators with a sensitive (subpicomolar sensitivity) proteomic tool to identify targeted residues. Mass spectrometry (MS) is a technique that allows separation and identification of ionized analyte molecules on the basis of their mass to charge ratio. In this study, we use MS to identify sites of TNM modification of the GlyR. After chemical labeling of reconstituted receptors, the receptors are denatured and subjected to proteolytic digestion to generate peptides with manageable molecular masses. Peptides may be identified by comparing the molecular mass of observed mass ions with predicted mass ions from the GlyR sequence, while a nitration by TNM yields a discernible mass shift (+45 mass units). The identity of the isolated mass ion can be further confirmed by collision-induced dissociation (CID) tandem MS (MS/MS), in which selected mass ions are fragmented into daughter ions. The mass difference between daughter ions in a series is indicative of the molecular mass of an amino acid. Thus, deconvolution of a daughter ion spectrum yields sequence information of the parent peptide. MS analysis provides a rapid and sensitive (under ideal conditions, femtomoles of peptide may be detected) means of identifying sites of TNM modification.

In this study, we have utilized the combination of chemical modification and mass spectrometry to examine the accessibility of Tyr residues of the GlyR in order to further refine the topology of this receptor. In addition to several tyrosine residues in the N-terminal domain, we have identified key tyrosine residues within M1 that are accessible to TNM modification. In particular, TNM modification of Tyr 223 and Tyr 228 suggests solvent accessibility at these sites, which conflicts with the four TM α-helix topological model that would place these residues buried within the lipid bilayer. These results corroborate a topological model in which the M1 region of the receptor cannot be entirely helical.

EXPERIMENTAL PROCEDURES

Sample Preparation and TNM Labeling. GlyR α1 homomers were overexpressed in Sf9 insect cells using a baculovirus expression system (*3*). Extraction, purification, and reconstitution of the receptor was performed as previously described (*4*). Briefly, GlyR was extracted from washed total membranes using a solubilization buffer containing 1% digitonin (Aldrich)/0.1% deoxycholate (Sigma) in 25 mM KP_i, pH 7.4, 1 M KCl, 5 mM EDTA, 5 mM EGTA, 10 mM DTT, and 1.5 mg/mL mixed lecithin (containing >99% phosphatidylcholine) (Calbiochem). Following affinity chromatography using 2-aminostrychnine−agarose, purified GlyR was reconstituted into lipid vesicles by size exclusion chromatography on Sephadex G-100. In our hands, this procedure reconstitutes GlyR in vesicles with native-like activity (*4*). A TNM (Sigma) stock solution of 6 mg/mL in 95% ethanol was stored at 4 °C under a blanket of N_2. Purified glycine receptor (200 μg) in phospholipid vesicles was bath sonicated in the presence of a 10−100-fold molar excess of tetronitromethane (TNM) in 25 mM KP_i, pH 7.4. The reaction was allowed to proceed for 1 h at room temperature. All reactions were stopped by addition of β-mercaptoethanol (βME) (Sigma) to a final concentration

of 5% (v/v) (*24*). Unreacted TNM and βME were removed by pelleting the GlyR vesicles via ultracentrifugation at 150000 × *g* for 1 h. The pellet was subsequently washed with reaction buffer, and ultracentrifugation was repeated. Samples of untreated GlyR were prepared under identical conditions as a negative control. The pellet was resuspended in electrophoresis buffer (1 M urea, 10% βME, 5% glycerol, bromophenol blue), and single bands were visualized on SDS−PAGE. GlyR bands were excised and proteolyzed "in-gel" with 1 μg of protease (trypsin or Endo-Glu-C) as described (*25*). Proteolytic fragments were extracted using 75% acetonitrile/100 mM acetic acid.

Estimation of TNM Labeling Efficiency. Samples of purified and reconstituted GlyR were labeled with TNM, centrifuged, and washed as described above. Pellets of TNM-reacted GlyR (10 μg) were resuspended in 10% acetonitrile/100 mM acetic acid (30 μL) and bath sonicated for 5 min. Samples were separated by C18 reverse-phase chromatography using a Waters Nova-Pak column (3.9 × 150 mm). Flow was driven by a Waters HPLC system including model 510 pumps and a model 996 photodiode array detector. Acquisitions and data analysis were performed using Millenium software (Waters). Unmodified GlyR eluted earlier than TNM-modified GlyR, confirmed by the presence of both peaks at 280 nm, but only the later peak absorbing at 428 nm. Labeling efficiency was inferred from measuring the peak area of modified GlyR at 280 nm.

HPLC Separation and Mass Spectrometry. Proteolytic fragments were separated using a Phenomenex reverse-phase column (C5, 150 × 46 mm, or C18, 50 × 0.3 mm) packed with 5 μm particles and a Waters model 600 HPLC system. Eluted proteolytic fragments were monitored by absorbance at 428 and 280 nm. Collected fractions were screened by ion-trap MS. Proteolytic fragments containing nitrated tyrosines were identified by running samples in parallel with control untreated GlyR. Mass ions unique to TNM-treated samples were assigned to the GlyR sequence. Theoretical masses of TNM-treated GlyR proteolytic fragments were generated using PAWS software (Proteometrics). Tentative assignments to the GlyR sequence were confirmed by MS/MS using a Fisons Quattro system, ESI triple-quadrupole MS, and/or a Finnigan LCQ ion-trap ESI-MS. Alternatively, data-dependent scans of selected mass ions monitored as they eluted from the LC were fragmented by CID using the Finnigan LCQ MS. The LC component was adapted with a flow splitter, which enabled reduction of precolumn flow from 200 to 20 μL/min.

RESULTS

Labeling of GlyR with TNM. Reconstituted GlyR was partially labeled with TNM. In our hands, the conditions used to reconstitute the receptor yield preparations in which the receptor effectively retains total activity (*4*), so any detected modifications by TNM of a specific GlyR residue are indicative of exposure to this aqueous reagent in native receptors. To limit the risk of artifactual labeling due to extended labeling times and/or local protein unfolding upon modification, labeling conditions were selected such that the receptor was only partially labeled. The efficiency of TNM labeling was monitored by exploiting the dramatic shift in retention time of the receptor upon TNM modification as observed by the appearance of a shifted absorbance at 428 nm (relative to the A_{280} peak of control reactions), the absorbance maximum of nitrotyrosine. Direct comparison of the A_{280} peak areas of modified and unmodified GlyR as peaks eluted from a C18 reverse-phase column indicated that approximately 40% of the protein remains unmodified by TNM under our conditions (data not shown). Thus, while a majority of our GlyR sample is labeled by TNM, after 1 h the reaction has not reached completion.

In the current study we utilized the sensitivity and versatility of mass spectrometry to identify TNM-labeled sites in GlyR. After labeling, the GlyR was proteolyzed by in-gel digestion with trypsin or Endo-Glu-C. Limit digests were then separated by reverse-phase HPLC. Given the necessity of lightly labeling the protein, we were not capable of detecting HPLC-separated proteolytic fragments containing *o*-nitrotyrosine residues by monitoring the absorbance of the eluant at 428 nm. Rather, direct infusion of HPLC fractions onto a Finnigan model LCQ ion-trap mass spectrometer was used to screen proteolytic fragments. Later, we adapted the LC component (Finnigan) of an LCQ ion-trap MS so that HPLC eluted proteolytic fragments could be analyzed directly by MS. Identification of TNM-labeled residues begins by comparing analogous HPLC fractions derived from modified and unmodified GlyR. In this fashion, peaks unique to the TNM-modified samples were tentatively assigned to the GlyR amino acid sequence and later confirmed by MS/MS. While TNM has been reported to have minor reactivity toward cysteine and tryptophan residues (*19*), these modifications were not detected under our experimental conditions. In our hands, all TNM labeling was found to occur solely at Tyr residues.

Representative MS/MS spectra are shown in Figures 1 and 2. Surprisingly, for several fragments, in addition to the expected mass shift of 45 Da (+NO_2) (Figure 2), a mass shift of 29 Da was also detected (Figure 1). We hypothesize that the 29 Da mass shift is the result of a loss of the tyrosyl oxygen during nitration (−16 mass units). Recently, similar losses of oxygen from nitrated tyrosine species were identified by MALDI-MS (*26*). Figure 1 illustrates MS/MS spectra for the parent mass ion 920.7, which was assigned to the sequence between GlyR residues 1 and 25. The spectra illustrated in panels A and B of Figure 1 were generated using lower (25%) and higher (35%) collision energies, respectively, yielding markedly different daughter ion species. Figure 1A is characterized by a strong parent mass ion peak at 920.1, suggesting that the efficiency of CID is low, and weak b and y ion series. Figure 1B has a significant reduction in the parent mass ion peak and a marked increase in the abundance of daughter ions due to the increased collision energy. Internal fragmentations caused by the presence of proline residues as well as presence of several b and y ions allow positive identification of this sequence assignment. Note that all b ions from both panel A and panel B in Figure 1 have a loss of 18 mass units, most likely due to the loss of a hydroxyl moiety, plus proton, from one of several serine residues. Figure 2 illustrates a MS/MS spectrum of the parent mass ion 779.5, obtained by triple-quadrupole ESI, which was assigned to the sequence between GlyR residues 223 and 234. In addition to a significant b and y ion series, this spectrum is marked by internal frag-

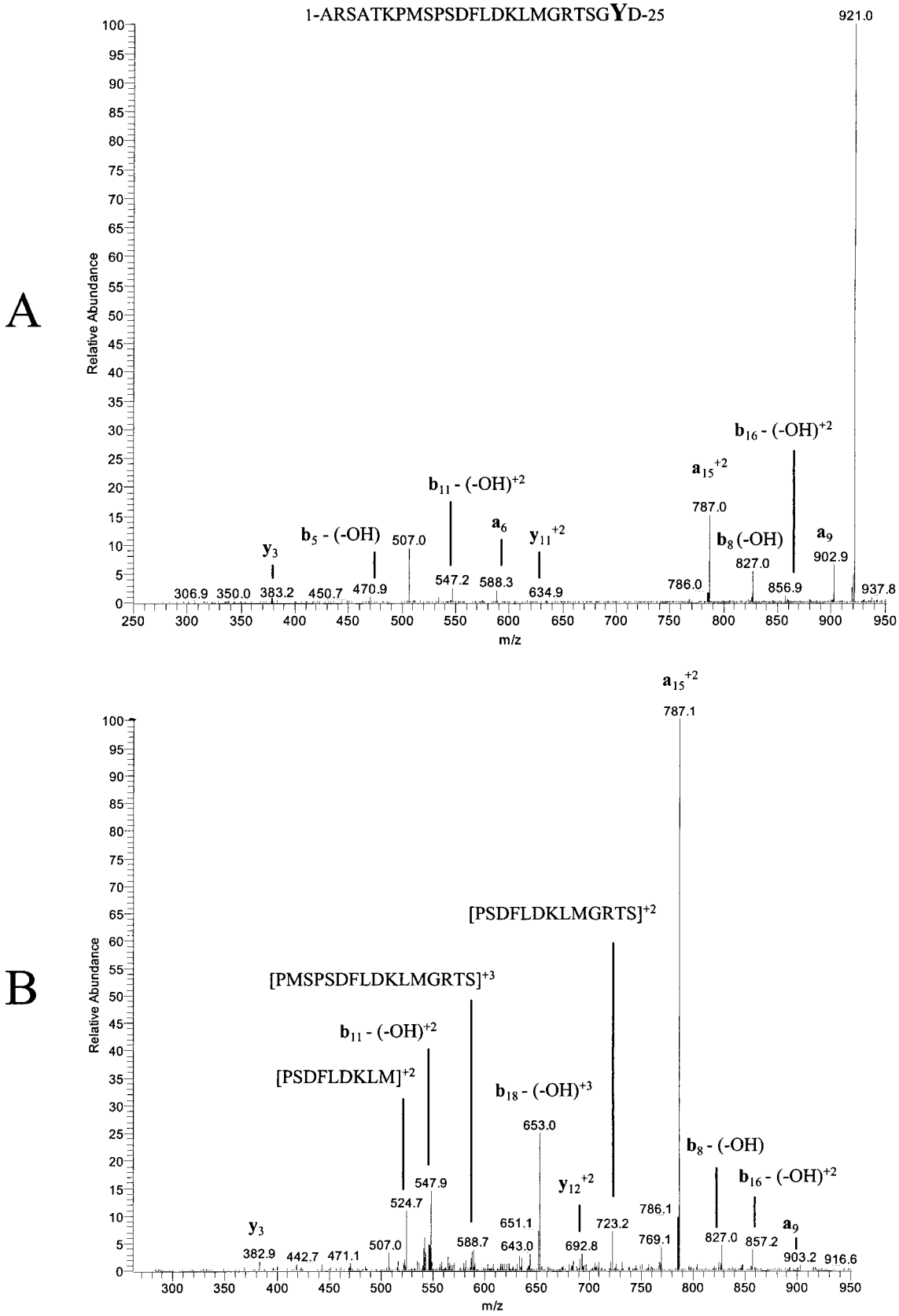

FIGURE 1: MS/MS spectra for parent mass ion 920.7 (GlyR proteolytic fragment 1−25). The MS/MS spectrum was acquired using a Finnigan LCQ LC ion trap. CID MS/MS spectra were generated by a data-dependent scan of the mass ion 920.7. (A) Collision energy set at 25% yielded spectra with lower yields of b, y, and a ions. (B) Collision energy set at 35% yielded spectra that included more internal "Pro" fragmentation that aided in the confirmation of sequence assignment.

ments induced by proline residues. Several daughter ions have a characteristic mass shift (−45 mass units), indicating that the nitrate moieties of *o*-nitrotyrosine residues are labile under CID MS/MS conditions.

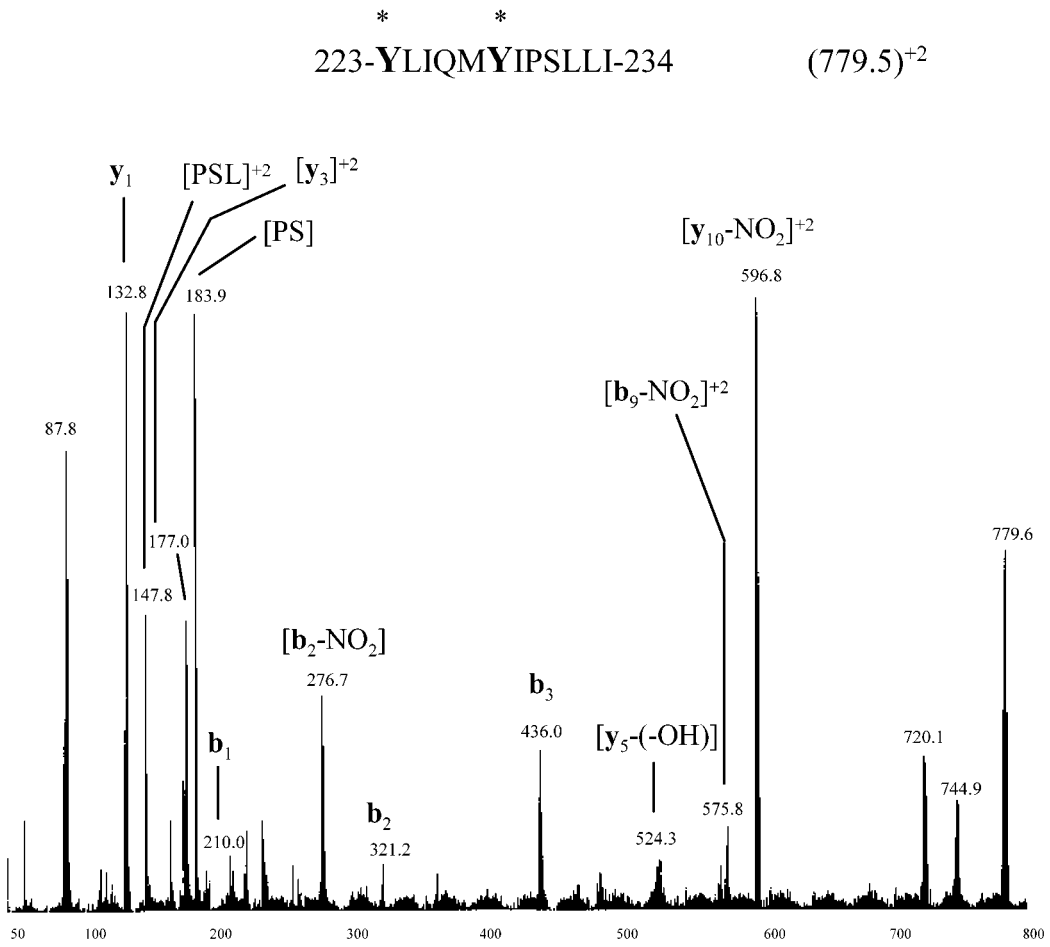

FIGURE 2: MS/MS spectrum for parent mass ion 779.5 (GlyR proteolytic fragment 223−234). The MS/MS spectrum was acquired by CID using a Fisons ESI triple-quadrupole MS. The molecular mass is consistent with two (NO_2−) moieties, which is confirmed by the sequence of the fragment. Loss of the (NO_2−) moieties by secondary fragmentation events are observed in b_2 and b_9 ions, as well as several internal fragments.

Table 1: Listing of Nitrated Tyrosine Residues Identified by MS Analysis[a]

NO_2−Y	proteolytic fragment	*M*/*z*	z	(M_{exp} − M_{obs})/*z*	
Y24	1−25	920.7	3	0.3	V8, 1/1 (+29)
Y24	16−25	1155.7	1	0.6	V8, 1/1 (+29)
Y75, Y78	54−81	907.1	4	0.4	V8, 2/3 (+45) × 2
Y75	71−77	890.6	1	0.3	V8, 1/1 (+29)
Y75, Y78	71−91	834.1	3	−0.9	V8, 2/2 (+29) × 2
Y78	78−81	537.4	1	0.1	V8, 1/1 (+29)
Y161	149−169	839.3	3	−1.3	V8, 1/1 (+29)
Y161	149−169	852.2	3	−1.2	V8, 1/1 (+29), K^+
Y223, Y228	223−234	779.5	2	−0.6	Tryp, 2/2 (+45) × 2
Y223	223−234	774.5	2	−1.4	Tryp, 1/2 (+45), K^+
Y228	223−234	756.1	2	−0.2	Tryp, 1/2 (+45)

[a]The proteolytic fragment that includes the modified tyrosine is also listed. The number of tyrosine residues labeled out of the total number of potential tyrosine residues within each proteolytic fragment is indicated as a ratio (i.e., 1/1 or 1/2). The exact modification is also noted as +45 for each nitrate moiety or +29, which is indicative of the loss of the nitrotyrosine oxygen. Abbreviations: V8, Endo-Glu-C; Tryp, trypsin; K^+, potassium adduct; *z*, charge; M_{exp}, expected mass; M_{obs}, observed mass.

FIGURE 3: GlyR α1 amino acid sequence with tyrosine residues highlighted in bold type. TNM-modified residues are underlined. The N-terminal domain sequence [aligned with AchBP (*27*)] is highlighted in gray.

Table 1 shows all of the proteolytic fragments of GlyR that were identified as containing TNM-modified tyrosine residues. Six of the 16 Tyr residues of α1 GlyR were modified. TNM modifications were detected in residues 24, 75, 78, 161, 223, and 228 (see Figure 4 for a schematic of the receptor and relative location of native tyrosines). Y58 lies within a fragment (54−81) that has a mass shift of 90 mass units, consistent with two nitration events. However, this fragment contains three tyrosine residues (58, 75, 78),

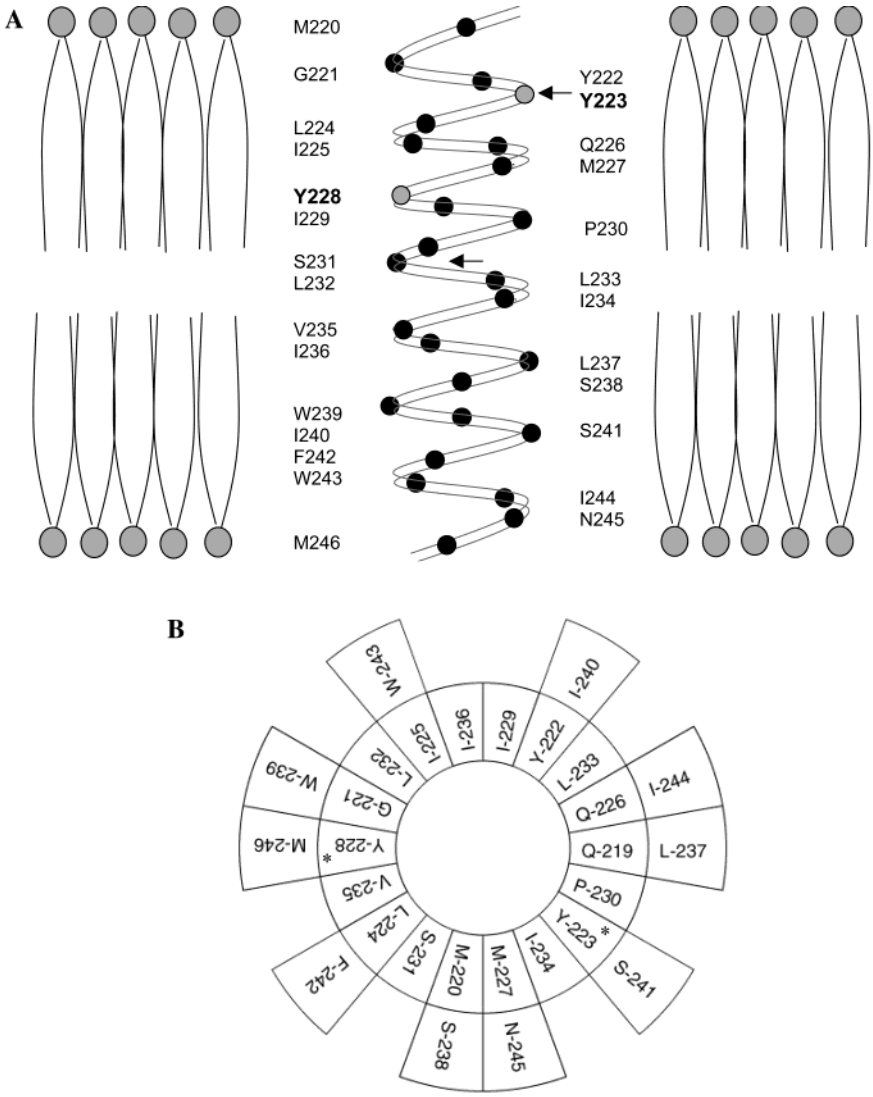

FIGURE 4: (A) Hypothetical schematic of GlyR residues 220−246 shown as a transmembranous α-helix. Individual residues are labeled along the length of the helix. Residues modified by TNM are shown as gray beads, and respective residue numbers are shown in bold type. Previously identified proteolytic cleavages (*5*) are indicated by arrows. (B) Helical wheel diagram (GROMACS v3.0) illustrating the relative position of M1 residues if this domain were to fold as an α-helix. TNM-modified residues are highlighted with asterisks.

only two of which are labeled. MS/MS of this fragment did yield sufficient daughter ions to determine the identity of the fragment; however, due to poor ionization, we were not able to verify the modification at Y58 (data not shown). Since modifications were detected associated with residues 75 and 78 (fragment 71−91), it was interpreted that Y58 is not modified by TNM. Except for tyrosine residues 223 and 228, all TNM modified tyrosine residues are located in the postulated N-terminal domain. Unexpectedly, nitration of tyrosine 339, located on the postulated cytoplasmic loop, was not observed. Similarly, nitration at tyrosine 301 was not detected. This residue flanks a proteolytic cleavage, identified in previous studies (*5*), and had been expected to be solvent accessible. Curiously, no modifications of any of the five Tyr C-terminal to residue 228 were detected. The absence of modification at these residues is difficult to interpret since the lack of labeling may not necessarily reflect a lack of accessibility to the aqueous milieu. While these residues may be inaccessible, it is also possible that they were labeled but remained undetected for a variety of reasons.

DISCUSSION

The current study utilizes chemical modification by TNM to probe the GlyR topology for solvent-accessible tyrosine residues. This type of approach had been useful in examining and refining the topology of the membrane protein bacteriorhodopsin (discussed further, below). By coupling this modification technique with mass spectrometry, we have been able to definitively identify 6 of the 16 native tyrosine residues in the GlyR as modified to *o*-nitrotyrosine in the presence of TNM. Coupled to our previous limited proteolysis study (*5*), these data provide further insight into the topology of the GlyR and, by homology, the nicotinicoid superfamily of ligand-gated ion channels.

N-Terminal Domain. Not surprisingly, several tyrosine residues located within the GlyR N-terminal domain (residues 1−218) were accessible for TNM modification (Table 1). Proteolytic peptides corresponding to residues 1−25 and 16−25 were mass shifted, allowing identification of Tyr 24 as a target of nitration by TNM. Similarly, peptide fragments encompassing Tyr 75 and/or Tyr 78 provided evidence of

their nitration. An additional proteolytic fragment (54−81) that includes tyrosine residues 58, 75, and 78 consistently yielded mass shifts which correspond to two nitration events (+90 mass units). However, we were never able to generate sufficient daughter ions to discern which tyrosine residue (besides Tyr 78) was nitrated, even though there were sufficient daughter ions to confirm the sequence assignment. Since we had detected modifications at Tyr 75 and Tyr 78 by other fragments, we interpreted that Tyr 58 was probably not modified by TNM. No modifications were detected at Tyr 128, Tyr 197, and Tyr 202.

Recently, a high-resolution structure of an acetylcholine binding protein (AchBP) secreted by snail glial cells has been determined (*27*). The sequence of this protein is highly homologous with the N-terminal domains of the nicotinicoid family of receptors, and more recent crystallographic data of bungarotoxin binding to a loop of the acetylcholine receptor suggest that the AchBP is structurally homologous with this domain of the nicotinicoid receptor (*28*). Therefore, the structure of this AchBP provides a useful framework in evaluating the structural information from our accessibility studies. Specifically, utilizing the sequence alignment provided in the Brejc study (*27*), we propose that the GlyR tyrosines might have accessibility profiles similar to their corresponding homologue in the AchBP structure. Four of the six GlyR Tyr residues that were identified as modified by TNM (24, 75, 78, 161) aligned with AchBP residues (S14, W65, H69, and H145, respectively); the other two labeled Tyr are in regions of the GlyR that is not homologous with AchBP. All TNM-modified GlyR residues, with the exception of Y161 (which is further discussed below), lie within solvent-accessible loops on the AchBP structure. Specifically, GlyR24−AchBP14 would be expected to be located at the C-terminal end of a short α-helix, and GlyR75 and GlyR78 would be located on the surface loop between two β-sheets (β2 and β3). Furthermore, alignment with AchBP suggests that the absence of labeling of Tyr 58, Tyr 128, Tyr 197, and Tyr 202 may be due to their inaccessibility rather than a failure of the methodology to detect these species. Tyr 58 and Tyr 128 of GlyR align with AchBP residues V48 and Y113, which both have side chains oriented to the hydrophobic interior of the β-barrel. Furthermore, Tyr 197 and Tyr 202 of GlyR align with AchBP residues N181 and C188. In AchBP these residues are in a Cys loop structure that is fairly hydrophilic and solvent accessible. However, in the nicotinicoid family of receptors, the loops on this surface of the N-terminal domain are not homologous to those in AchBP but rather are generally hydrophobic and may be involved in protein−protein interactions with other surface loops of the full-length receptor. As such, the Tyr at 197 and 202 might not be accessible to aqueous reagents and would remain unmodified by TNM.

The observed TNM modification of Tyr 161 suggests solvent accessibility at this site. Mutagenesis studies of GlyR have identified residues 159, 160, and 161 as critical in agonist/antagonist binding and specificity (*31, 32*). Therefore, Tyr 161 is involved in ligand binding and might be expected to be accessible to aqueous TNM. However, how do we accommodate this with our previous limited proteolysis studies that identified the proteolytic 158−165 peptide as partitioning with the membrane-associated components after proteolysis (*18*)? In sequence alignments with the AchBP, GlyR Y161 is homologous to AchBP H145, which lies at the interface between subunits of the AchBP pentamer. Strong noncovalent interactions between neighboring subunits in the 158−165 region of GlyR would result in membrane association of the peptide with an intact neighboring subunit. Our results are consistent with a model in which Tyr 161 is part of the ligand binding site at the interface between neighboring subunits.

Transmembrane M1 Region. TNM modifications were identified at residues 223 and 228 of M1, suggesting solvent accessibility at sites that should have been occluded from modification if M1 were to fold as a "classical" TM α-helix (Figure 4). Even if the side chains of portions of this helix were partially lining the pore channel, we would not expect tyrosine residues 223 and 228 to have access to water-soluble reagents and would expect them to be on different faces of an α-helix (see helical wheel in Figure 4B). This result is consistent with accessibility patterns observed in the M1 domain of the homologous nAchR by other investigators. Karlin and co-workers have used extensive systematic cysteine mutagenesis coupled with covalent modification using aqueous methanethiosulfonate compounds to probe the structure of the M1 and M2 regions of nAchR (*12, 13*) (see ref *29* for an overview). The labeling patterns of the amino-terminal end of the M1 regions of both the α and β subunits of the nAchR were inconsistent with this area being α-helical, and it has been postulated that this region lacks regular structure and these side chains may be accessible to solvent in the pore of the channel. In addition, biochemical data (*9*), involving the use of various probes with the AchR, have failed to produce convincing evidence that M1 folds entirely as a transmembrane α-helix, and we interpret the labeling pattern of these hydrophobic probes as being consistent with a nonhelical structure (for a review see ref *30*). Fluorescence quenching experiments with AchR suggest that Cys 222 [corresponding, by sequence alignment, to GlyR residue 231 (*31*)] lies closer to the membrane−solvent interface than the hydrophobic interior of the bilayer (as would be suggested if M1 were α-helical). Given all this evidence, we consider an alternate hypothesis: if, as many investigators have shown, the M1 domain is not entirely helical, is it not more plausible that some of these accessible residues are located on surface loops near the interfacial region of the bilayer?

The domains of integral membrane proteins that face the hydrophobic interior of the lipid bilayer must somehow satisfy the hydrogen-bonding requirements of the carbonyl and amide moieties of the peptide bonds. The energy of desolvating these moieties upon transfer to a hydrophobic environment is the single most important driving force in membrane protein folding (*26*). TM domains are therefore typically assumed to form regular secondary structures (α-helix or β-sheets) in which carbonyl groups and amide groups may form hydrogen bonds (intrachain or interchain, respectively) and reach a stable thermodynamic energy state. Typically, TM α-helices require no less than 20 amino acids to traverse the approximately 30 Å of the hydrocarbon interior of the lipid bilayer. However, as indicated by the porin crystal structure (*32*), TM β-sheets may span the bilayer with as few as six residues. Therefore, biochemical studies that employ the use of proteases or chemical modification

reagents with specific solubilities have been very useful in defining the limits of TM domains. Thus, the length of the TM domains strongly delimits the possible secondary structure of these TM domains (i.e., transmembrane stretches of less than 20 amino acids cannot be entirely helical and pass through the bilayer).

If we postulate that the transmembrane domain of M1 is comprised of multiple β-sheets satisfying their H-bonds by interstrand bonding (with adjacent strands from other subunits), then we are not limited to a single pass through the bilayer. If M1 traverses the bilayer as multiple β-sheets, it must fold as an odd number of β-sheets in order to preserve the vectorial orientation of M2 (*8*). We have previously identified proteolytic cleavages, under native conditions, at GlyR residues 223 and 234, suggesting solvent accessibility at these sites that is not consistent with an α-helical fold for this region (*5*). As described above, identification of TNM modification at GlyR residues 223 and 228 also suggests that M1 is unlikely to fold as a membrane-spanning α-helix but may instead be comprised of an odd number of β-sheets where several residues between 220 and 246 are solvent accessible. Analogous TNM modification studies conducted on bacteriorhodopsin (BR) showed that this technique was capable of labeling Tyr in the interfacial region of the membrane (*20*, *33*). Significantly, BR tyrosine residues buried within the bilayer could not be nitrated by TNM under similar experimental conditions. Thus, Tyr 223 and/or Tyr 228 of GlyR may reside in the interfacial region of the bilayer and remain accessible to nitration by TNM, but they cannot be buried in the hydrophobic interior of the bilayer and may define the ends of a transmembrane β-sheet.

The recent determination of the high-resolution structures of the glycerol-conducting aquaporin (GlpF) (*34*) and the ClC channel (*35*), two membrane channels, suggests yet another possibility for the topology of the nicotinicoid family. Surprisingly, the crystal structures of these two membrane proteins have significant amounts of membrane-embedded residues which are neither entirely helical nor in β-sheets. Similar to the KcsA channel (*36*), these proteins have helices that only penetrate partially through the membrane. Perhaps the M1 region of the nicotinicoid receptor superfamily (and, quite possibly, other regions of the receptor) similarly contains a novel, unexpected secondary structure. While the TNM labeling data presented herein cannot define the secondary structure on M1, the data strongly suggest that this domain cannot be entirely helical. Our laboratory is currently utilizing cysteine substitution mutagenesis coupled to spin-labeling techniques to further probe the local environment of this region.

In conclusion, TNM modification coupled with mass spectrometric studies has been shown to be a useful tool in examining membrane protein topology. Labeling of the GlyR at various sites in the N-terminal domain is consistent with their expected accessibility. Previous studies suggested that Tyr 161 is involved in ligand binding, and its accessibility to TNM was consistent with these studies. However, TNM modification of two tyrosine residues in M1 lends support to findings from a previously published study suggesting that the TM1 region of the nicotinicoid receptors might not be α-helical. Specifically, nitration at tyrosine residues 223 and 228 of GlyR indicates that these residues have access to the aqueous milieu and strongly suggests that M1 cannot fold as a transmembrane α-helix, which would place these residues well within the lipid bilayer.

ACKNOWLEDGMENT

We thank Brian Gribble for outstanding technical support, Dr. Andrew Amoscato (University of Pittsburgh School of Medicine) for ESI triple-quadrupole MS support, and Dr. Mark Bier (Carnegie Mellon University, Center for Molecular Analysis) and Dr. Mona Shahgholi (California Institute of Technology) for LCQ ion-trap MS support.

REFERENCES

1. Schmieden, V., Grenningloh, G., Schofield, P. R., and Betz, H. (1989) *EMBO J. 8*, 695−700.
2. Sontheimer, H. B. C., Pritchett, D. B., Schofield, P. R., Grenningloh, G., Kettenmann, H., Betz, H., and Seeburg, P. H. (1989) *Neuron 2*, 1491−1497.
3. Cascio, M., Schoppa, N. E., Grodzicki, R. L., Sigworth, F. J., and Fox, R. O. (1993) *J. Biol. Chem. 268*, 22135−22142.
4. Cascio, M., Shenkel, S., Grodzicki, R. L., Sigworth, F. J., and Fox, R. O. (2001) *J. Biol. Chem. 276*, 20981−20988.
5. Leite, J. F., Amoscato, A., and Cascio, M. (2000) *J. Biol. Chem. 275*, 13683−13689.
6. Apel, E. D., Roberts, S. L., and Campbell, K. P. (1995) *Neuron 15*, 115−126.
7. Meyer, G., Kirsch, J., and Betz, H. (1995) *Neuron 15*, 563−572.
8. Corringer, P. J., Le Novere, N., and Changeux, J. P. (2000) *Annu. Rev. Pharmacol. Toxicol. 40*, 431−458.
9. Blanton, M. P., and Cohen, J. B. (1994) *Biochemistry 33*, 2859−2872.
10. Blanton, M. P., Dangott, L. J., Raja, S. K., Lala, A. K., and Cohen, J. B. (1998) *J. Biol. Chem. 273*, 8659−8668.
11. White, B. H., and Cohen, J. B. (1988) *Biochemistry 27*, 8741−8751.
12. Akabas, M. H., Kaufmann, C., Archdeacon, P., and Karlin, A. (1994) *Neuron 13*, 919−927.
13. Akabas, M. H., and Karlin, A. (1995) *Biochemistry 34*, 12496−12500.
14. Görne-Tschelnokow, U., Strecker, A., Kaduk, C., Naumann, D., and Hucho, F. (1994) *EMBO J. 13*, 338−341.
15. Ortells, M. O., L. G. (1996) *Protein Eng. 9*, 51−59.
16. Methot, N. R. B., Blanton, M. P., and Baenziger, J. E. (2001) *J. Biol. Chem. 276*, 23726−23732.
17. Unwin, N. (1992) *J. Mol. Biol. 229*, 1101−1124.
18. Miyazawa, A., Fujiyoshi, Y., Stowell, M., and Unwin, N. (1999) *J. Mol. Biol. 288*, 765−786.
19. Sokolovsky, M., Riordan, J. F., and Vallee, B. L. (1966) *Biochemistry 5*, 3582−3591.
20. Lemke, H. D., and Oesterhelt, D. (1981) *Eur. J. Biochem. 115*, 595−604.
21. Scherrer, P. S. W. (1984) *Biochemistry 23*, 6195−6202.
22. Luecke, H., Schobert, B., Richter, H. T., Cartailler, J. P., and Lanyi, J. (1999) *J. Mol. Biol. 291*, 899−911.
23. Ladokhin, A. S., and White, S. H. (2001) *J. Mol. Biol. 309*, 543−552.
24. Lilova, A., Kleinschmidt, T., Nedkov, P., and Braunitzer, G. (1986) *Biol. Chem. Hoppe-Seyler 367*, 861−870.
25. Zhou, J., Rusnack, J. F., Colonius, T., and Hathaway, G. M. (2000) *Rapid Commun. Mass Spectrom. 14*, 432−438.
26. Sarver, A. S. N., Shetlar, M. D., and Gibson, B. W. (2001) *J. Am. Soc. Mass Spectrom. 12*, 439−448.
27. Brejc, K., van Dijk, W. J., Klaassen, R. V., Schuurmans, M., van der Oost, J., Smit, A. B., and Sixma, T. K. (2001) *Nature 411*, 269−276.
28. Harel, M., Kasher, R., Nicolas, A., Guss, J. M., Balass, M., Fridkin, M., Smit, A. B., Brejc, K., Sixma, T. K., Katchalski-Katzir, E., Sussman, J. L., and Fuchs, S. (2001) *Neuron 32*, 265−275.

29. Karlin, A. (2002) *Nat. Rev. Neurosci. 3*, 102−114.
30. Leite, J. F., and Cascio, M. (2001) *Mol. Cell. Neurosci. 17*, 777−792.
31. Kim, J., and McNamee, M. G. (1998) *Biochemistry 37*, 4680−4686.
32. Buchanan, S. K. (1999) *Curr. Opin. Struct. Biol. 9*, 455−461.
33. Fimmel, S., Choli, T., Dencher, N. A., Buldt, G., and Wittman-Liebold, B. (1989) *Biochim. Biophys. Acta 978*, 231−240.
34. Fu, D., Libson, A., Miercke, L. J., Weitzman, C., Nollert, P., Krucinski, J., and Stroud, R. M. (2000) *Science 290*, 481−486.
35. Dutzler, R., Campbell, E. B., Cadene, M., Chait, B. T., and MacKinnon, R. (2002) *Nature 415*, 287−294.
36. Doyle, D. A., Morais Cabral, J., Pfuetzner, R. A., Kuo, A., Gulbis, J. M., Cohen, S. L., Chait, B. T., and MacKinnon, R. (1998) *Science 280*, 69−77.

BI015895M